



## The impact of electrical stimulation on NaCl diffusion in tenderloin and the quality of dry-cured loin during the marination process

Mixin Zhou<sup>a,b</sup>, Yuanyuan Liu<sup>a,b</sup>, Chun Ye<sup>a,b</sup>, Linggao Liu<sup>a,b</sup>, Li Chen<sup>a,b</sup>, Lisha Lan<sup>a,b</sup>, Shenghui Bi<sup>a,b</sup>, Yehua Liu<sup>a,b</sup>, Keshan Wang<sup>a,b</sup>, Minfei Liu<sup>a,b</sup>, Qiujin Zhu<sup>a,b,c,\*</sup>

<sup>a</sup> School of Liquor and Food Engineering, Guizhou University, Guiyang 550025, China

<sup>b</sup> Key Laboratory of Agricultural and Animal Products Store and Processing of Guizhou Province, Guiyang 550025, China

<sup>c</sup> Key Laboratory Mountain Plateau Animals Genetics and Breeding, Ministry of Education, Guiyang 550025, China

### ARTICLE INFO

#### Keywords:

Electrical stimulation  
Mass transfer  
NaCl penetration  
Energy dispersive spectrum  
Meat quality

### ABSTRACT

The effects of electrical stimulation (ES) during the post-processing stage on NaCl diffusion, microstructure, and overall quality in the dry curing of pork tenderloin were investigated. ES treatment significantly increased the salt content in pork tenderloin, with the A2ES group (ES applied after 2 h of curing) showing a 28.32 % increase compared to the control group. Energy spectrum analysis revealed that NaCl distribution in the meat tissue was most concentrated following ES treatment. Binarized images of NaCl permeation in pork loin clearly demonstrated that ES enhanced NaCl permeation. Additionally, microscopic analysis showed that ES caused cell disintegration, and the combined effect of ES and NaCl damaged muscle tissue. The results indicate that ES enhanced NaCl diffusion and shortened the curing time, while improving meat tenderness and reducing bitter and astringent flavors. This study offers new insights and techniques to accelerate the marination process of meat products.

### 1. Introduction

Curing is a traditional method of meat processing that has been utilized for centuries to preserve meat, extend its shelf life, and enhance its flavor. The material changes and mass transfer processes in meat curing primarily involve the diffusion of solutes, such as sodium chloride (NaCl), as well as the penetration of water (Ye et al., 2023). NaCl redistribution occurs through two distinct pathways: first, via the surface membranes of meat tissue; second, through the capillary system within the intercellular spaces of muscle tissue (Graiver et al., 2009). Sodium chloride not only imparts a salty taste to food, enhancing the flavor and texture of meat, but also inhibits the growth of spoilage microorganisms, thereby extending the shelf life of meat products.

The complex structure of myogenic fibers, intramuscular fat, and the barrier effect of cell membranes limit NaCl diffusion during traditional curing. This results in a particularly time-consuming process for salt to diffuse from the surface into the muscle. Salt diffusion is significantly affected by changes in muscle structure and membrane permeability. Therefore, accelerating the curing process by manipulating muscle structure and membrane permeability is a key objective (Janositz et al.,

2011). In recent years, several innovative techniques have been developed to enhance the efficiency of curing. One such technique is ultrasonic-assisted curing, which uses ultrasound waves to disrupt the cell membrane structure in pork tissues, thereby increasing the NaCl content in the meat (Guo et al., 2024). Vacuum curing of cod promotes salt diffusion and reduces processing time by 75 % (Tomac et al., 2020). Synchronized ultrasound-assisted marination at varying frequencies alters the meat's microstructure, facilitating NaCl penetration and enhancing pork quality (Guo et al., 2023). The application of a pulsed electric field during marination disrupts cell membrane permeability, enlarging the gaps between muscle bundles and effectively reducing marination time (Zhang et al., 2022). However, existing reports on NaCl mass transfer have focused primarily on the wet curing process, with limited studies on the dry curing process.

Electrical stimulation (ES), a physical technique utilizing an electric field, is primarily used for meat tenderization in pre-slaughter treatments. This process has the potential to enhance muscle brightness (Sleper et al., 2006). Low-voltage electrical stimulation has been shown to significantly impact various biochemical indices related to meat, including pH, glycolysis, and enzyme activities (Zhao et al., 2022).

\* Corresponding author at: School of Liquor and Food Engineering, Guizhou University, Guiyang 550025, China.

E-mail address: [ls.qjzhu@gzu.edu.cn](mailto:ls.qjzhu@gzu.edu.cn) (Q. Zhu).

<https://doi.org/10.1016/j.fochx.2024.102000>

Received 2 September 2024; Received in revised form 9 November 2024; Accepted 11 November 2024

Available online 14 November 2024

2590-1575/© 2024 The Authors. Published by Elsevier Ltd. This is an open access article under the CC BY-NC-ND license (<http://creativecommons.org/licenses/by-nc-nd/4.0/>).

Medium-pressure electrical stimulation has been shown to significantly enhance the tenderness of meat products without adverse effects (Biffin et al., 2018). Some studies suggest that ES can reduce the lengthy processing cycle of dry-cured ham and improve protein utilization (Yue et al., 2024). Additionally, ES treatment increased NaCl content in dry-cured tenderloins (Zhang et al., 2024). Studies have shown that current treatment can compromise the integrity of the plasma membrane, alter its permeability, and ultimately result in electrical breakdown (Saulis, 2010), thus improving the mass transfer capacity. Currently, electrical stimulation (ES) is primarily utilized for slaughtering and tenderizing meat. While our team has researched the use of ES in marination and post-processing stages, there is limited information on its application in meat post-processing overall. Furthermore, the ES equipment employed in livestock slaughtering lines uses transistor conduction to regulate the heating devices. Although the technical requirements are relatively straightforward, there is a lack of precise control over the operating time of the electrodes. Additionally, the single waveform and the parameters for regulation, precision, and intelligence are not highly advanced. Currently, meat electrical stimulation (ES) equipment technology lags significantly behind that of engineering medicine. To enhance the theory and application of ES in meat processing, more sophisticated ES equipment is essential.

In conclusion, this study utilized AC power from a programmable supply with precise measurement capabilities to treat pork tenderloin. The impact of ES on NaCl diffusion in dry-cured tenderloin during the post-processing stage was investigated, along with its effect on cell membrane permeability, characterized through the cell disintegration index, the diffusion coefficient of NaCl in the dry-curing process of tenderloin was calculated using Fick's second law ( $De$ ). A mathematical model was constructed to elucidate the effect of ES on the mass transfer driving force. Additionally, the diffusion process and distribution of NaCl in the loin were visualized using the food dye penetration method and energy spectrum analysis. Furthermore, changes in the tissue microstructure of pork after ES treatment were observed. Additionally, the quality and flavor of ES-treated dry-marinated pork loin were evaluated using quality indices such as pH, shear force, texture, color, and electronic tongue, to assess the potential of ES application in the post-processing stage.

## 2. Materials and methods

### 2.1. Materials

The pork tenderloin was supplied by Guizhou Tainong Xingwang Food Co., Ltd. (Guiyang, China). Fresh pork tenderloins from slaughtered pigs were transported to the laboratory in insulated ice boxes, with a total sample size of 240. The pH of three different parts of the pork loin was tested using a calibrated portable meat-specific puncture pH meter (Testo 205, Testo SE & Co. KGaA, Germany). After removing subcutaneous fat and connective tissue from pork tenderloin with pH range of 5.6–6.0, parallel samples (40 mm × 30 mm × 10 mm, weighing 15 ± 1 g) were taken from myogenic fibers with a sharp knife, weighed and recorded, and then placed in a refrigerator at 4 °C for backup. The initial salt content of the raw meat was measured to be 0.05 ± 0.01 g/100 g, and 71.68 ± 0.21 g/100 g meat of water.

### 2.2. ES processing cure

ES processing equipment is AFV-P series (AFV-P600, Preen Power Supply Co., Ltd., Suzhou, China). The AFV-P series is a programmable AC power supply with DC output and precise measurement functions to provide pure AC power during processing. Processing method reference (Zhang et al., 2024) with slightly modified, add sodium chloride to the tenderloin at a material ratio of 3 %, evenly coated with NaCl, then vacuumed and placed in a static marinade in a cold room at 4 °C. The myofibrillar fibers of the sample were in contact with the aluminum

electrode plate, with a current of 0.9 A applied for a treatment duration of 90 s. The sample treatment is illustrated in Fig. 1. The samples were divided into five groups: a control group that was marinated without any treatment (CK), and four groups subjected to electrical stimulation (ES) at different times: before the start of curing (BES), after 2 h of curing (A2ES), after 8 h (A8ES), and after 12 h (A12ES). Static curing was then continued for 24 h. Samples were collected at 1, 2, 4, 8, 12, 18, and 24 h of dry curing, with all samples taken in triplicate for subsequent analysis.

### 2.3. Determination of cell disintegration index

The disintegration index ( $Z$ ), based on conductivity measurements, is a method used to assess the effect of electric fields on food ingredients. It quantifies the degree of disintegration and damage to cell membranes caused by electric fields (Lebovka et al., 2002). The conductivity of the samples before and after electric field treatment was measured using a conductivity meter, and the value of  $Z$  was calculated using eq. (1):

$$Z = \frac{(\sigma - \sigma_i)}{(\sigma_d - \sigma_i)} \quad (1)$$

here,  $\sigma$  represents the conductivity ( $\text{mS}\cdot\text{cm}^{-1}$ ) of the ES-treated sample,  $\sigma_i$  represents the conductivity ( $\text{mS}\cdot\text{cm}^{-1}$ ) of the intact sample, and  $\sigma_d$  represents the conductivity ( $\text{mS}\cdot\text{cm}^{-1}$ ) of the completely destroyed sample after being frozen twice at  $-20$  °C and thawed at room temperature within 48 h. The measurements were repeated three times, and the mean and standard deviation were calculated.

### 2.4. Determination of NaCl content

Following the method described by (Liu et al., 2022) with slight modifications, the NaCl content of the samples was determined in triplicate using a calibrated mini digital salinometer (PAL-SALTPROBE, ATAGO, Tokyo, Japan). One gram of the meat sample was diluted tenfold with deionized water and homogenized for 10 s. The NaCl content was expressed as grams per 100 g of meat.

### 2.5. Determination of weight and moisture content

The sample is removed and weighed. Moisture content is measured by cutting 2 g of sample accurately, chopping it and placing it in an oven at 105 °C until the weight remains constant (Guo et al., 2024).

### 2.6. Mass transfer kinetics

During the curing process, the primary material exchanges between the pork tenderloin and salt were NaCl diffusion and water osmosis, with trace amounts of fat and protein being insignificant. The change in mass of the tenderloin is proportional to the square root of time, as demonstrated by the following eq. (2):

$$\Delta M_t^i = 1 + K_1 + K_2 \times t^{0.5} \quad (2)$$

where  $K_1$  and  $K_2$  are the kinetic parameters;  $K_1$  represents the initial situation of the curing process;  $K_2$  is related to the mass transfer drive;  $\Delta M_t^i$  including change in total weight ( $\Delta M_t^0$ ), change in moisture content ( $\Delta M_t^w$ ) and change in NaCl content ( $\Delta M_t^{\text{NaCl}}$ ) respectively, it can be calculated by the following formula (3) (4) (5):

$$\Delta M_t^0 = \frac{M_t^0 - M_0^0}{M_0^0} \times 100 \quad (3)$$

$$\Delta M_t^w = \frac{M_t^0 \times X_t^w - M_0^0 \times X_0^w}{M_0^0} \times 100 \quad (4)$$

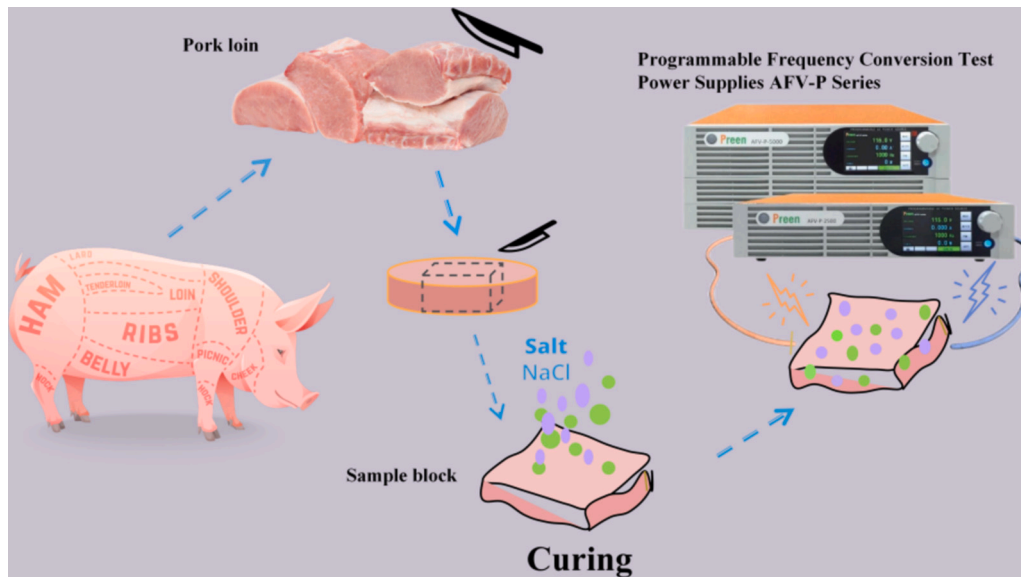


Fig. 1. Sample processing.

$$\Delta M_t^{NaCl} = \frac{M_t^0 \times X_t^{NaCl} - M_0^0 \times X_0^{NaCl}}{M_0^0} \times 100 \quad (5)$$

where:  $M_t^0$  and  $M_0^0$  represent the weight of the loin (g) at the time of dry curing  $t$  and  $0$ , respectively;  $M_t^W$  and  $M_0^W$  represent the moisture content of the loin (%) at the time of dry curing  $t$  and  $0$ , respectively;  $X_t^{NaCl}$  and  $X_0^{NaCl}$  represent the NaCl content of the loin (%) at the time of dry curing  $t$  and  $0$ , respectively.

## 2.7. Calculation of NaCl diffusion coefficient ( $De$ )

The diffusion coefficient ( $De$ ) of NaCl during the dry curing process was determined using Fick's second law to characterize the change in NaCl content (Ozuna et al., 2013). In the model, it was assumed that the sample was a regular rectangular body and that the diffusion of NaCl was a simple unidirectional osmosis (Nguyen et al., 2010).  $De$  was calculated by the following eq. (6):

$$1 - Y_t^{NaCl} = 1 - \left[ \frac{(z_t^{NaCl} - y_t^{NaCl})}{(z_0^{NaCl} - z_e^{NaCl})} \right] = 2 \times \left( \frac{De \times t}{\pi \times L^2} \right)^{0.5} + K \quad (6)$$

where:  $Y_t^{NaCl}$  is the driving force for the reduction between the aqueous phase and the exudate in the dry-cured ridges;  $Z_t^{NaCl}$  is the mass fraction of NaCl in the aqueous phase of the ridges at the moment  $t$  of dry-curing;  $y_t^{NaCl}$  is the mass fraction of NaCl in the exudate at the moment  $t$  of dry-curing;  $Z_0^{NaCl}$  is the mass fraction of NaCl in the aqueous phase of the ridges at the moment  $0$  of dry-curing;  $Z_e^{NaCl}$  is the mass fraction of NaCl in the aqueous phase of the ridges when equilibrium is reached by dry-curing;  $De$  ( $m^2/s$ ) is the effective diffusion coefficient ( $De(m^2/s)$  is the effective diffusion coefficient;  $t$  is the curing time;  $L$  is half the thickness of the sample;  $K$  is a constant, with the help of which any thermodynamic mechanism or other mass transfer phenomenon effect at the beginning of the curing can be corrected.

## 2.8. Measurement of NaCl permeability

Penetration of NaCl in tenderloin with slight modifications in reference to (Liu et al., 2010). Food dye powder FD&C Blue No.1 (Henan Xinxiang Kexing Additives Co., Ltd., Henan, China) at a content of 0.1 % was added to 3 % NaCl and mixed well to form a marinade with dye penetration, curing is handled in accordance with Section 2.2. After

curing, the osmotic liquid on the surface should be dried, and the sample should be frozen and stored at  $-18^\circ C$  for 4 h. The sample is then sliced into 2 mm thick sections along the center, parallel to the myofibrils. Sample sections were photographed with a Canon camera (Canon 200D II, Canon Corporation, Japan), and the RGB images were converted to grayscale using the Red Channel to Grayscale method. Binarization was then performed following automatic threshold segmentation. Rectangular areas (pixel size:  $720 \times 220$ ) were cropped to characterize dye distribution. The amount of NaCl penetration along the longitudinal direction of the myofibrils in the loin was quantified by calculating the percentage of the dye penetration area relative to the total.

## 2.9. Energy dispersive spectroscopy (EDS) combined with scanning electron microscopy (SEM) analysis

Fresh meat (FS) and cured meat samples (CK, BES, and A2ES groups) were sliced into 1 mm thick sections, flash-frozen in liquid nitrogen, and then freeze-dried for 24 h using a vacuum freeze-dryer (FD-1 A-50, Jinan Boyikang, China). The samples were then directly attached to conductive adhesive, coated with gold, and subsequently analyzed using a scanning electron microscope (ZEISS GeminiSEM 300, Germany) equipped with EDS and SE2 secondary electron detectors to capture the sample morphology and perform energy spectrum mapping. The distribution of sodium and chloride ions in the flake samples was also analyzed.

## 2.10. Light microscopy observation

Paraffin sections were prepared using the method described by (Wu et al., 2022) with slight modifications. The dry-cured samples were pickled and cut into rectangular columns ( $1 \times 1 \times 1 \text{ cm}^3$ ) before being fixed in 4 % paraformaldehyde for over 24 h. Dehydration was then performed sequentially with graded alcohols: 65 %, 75 %, 90 %, 95 %, and 100 %. The wax-impregnated tissue was embedded, cooled, and then sliced into 3–4  $\mu m$  thin sections. The microstructure of the porcine tenderloin was visualized using hematoxylin-eosin (H&E) staining and observed with a scanner (Gemini AS, 3D, Germany).

## 2.11. Evaluation of the quality of ES processing

Measuring pH with a portable meat-specific puncture pH meter (Testo 205, Testo SE & Co. KGaA, Germany). The test of texture is based

on the method (Ozuna et al., 2013) with slightly modified. Remove the dry-cured sample and place it in a sealed cooking bag. Submerge the bag in a water bath maintained at 80 °C. Insert a probe thermometer into the center of the tenderloin until the internal temperature reaches 80 °C. The sample is then cooled to room temperature, and a 1 cm<sup>3</sup> sample is cut from the center of the meat. Subsequently, the hardness, elasticity, and chewability of the samples were evaluated using a texture analyzer (CT3, Beaufepley, USA), the probe used is the TA/36, parameterized to 1.0 mm/s pre-test, 1.0 mm/s mid-test, 1.00 mm/s post-test, and 50 % compression ratio. Determination of tenderness is based on the method of (Ye et al., 2023) with slight modification. The samples were cut into 1 cm<sup>3</sup> and tested perpendicular to the direction of muscle fibers using a digital muscle tenderness meter (C-LM3B, Northeastern Agricultural University, China), with the shear speed set at 5 mm/s. Color was measured using a convenient computerized colorimeter (NH350 Agilent, Shenzhen Sanenshi Technology Co., China) for colorimetric measurements, and samples of dried marinated tenderloin were cut into uniform slices to measure brightness (L\*), redness (a\*), and yellowness (b\*). Calculate E\* according to Eq. (7) (X. Zhang et al., 2024).

$$E^* = \frac{a^*}{L^*} + \frac{b^*}{L^*} \quad (7)$$

where, a\* represents the redness value, L\* represents the brightness value, and b\* represents the yellowness value.

## 2.12. Electronic tongue measurements

Forty milliliters of distilled water and 10 g of chopped meat samples were mixed and homogenized at 4500 rpm for 40 s using a homogenizer (XHF-DY, Xinzhi Biotechnology Co., Ltd., Ningbo, China). The supernatant was then centrifuged at 2000g for 10 min at 4 °C and filtered

through filter paper. Next, 10 mL of the sample solution was mixed with 50 mL of ultrapure water using a two-step washing method to evaluate the flavor on an SA 402 B electronic tongue (Insent, Kanagawa, Japan) (Liu et al., 2022). The reference solution consisted of 30 mM potassium chloride and 0.3 mM tartaric acid.

## 2.13. Statistical analysis

All experiments were conducted in at least triplicate, with data expressed as mean ± standard error (SE) and analyzed using analysis of variance (ANOVA) with SPSS 25.0 (SPSS Inc., IL, USA). The presence of significant differences between experiments was assessed using Tukey's test, with statistical significance set at  $p < 0.05$ . Plots were generated using Origin 2021 (OriginLab Corporation, MA, USA).

## 3. Results and discussion

### 3.1. Effect of ES-mediated marination on NaCl content in tenderloins

Fig. 2(A) illustrates the NaCl content in pork tenderloins after electrical stimulation (ES) at different stages of dry curing. Both the control group (CK) and the ES group exhibited an increasing trend in NaCl content with extended dry curing time. In the early stage of marination, the high NaCl concentration in the external environment and the relatively low concentration within the loin create a significant osmotic pressure difference. This causes continuous water exudation from the loin. The water, combined with the salt particles on the surface, forms a sodium chloride solution that diffuses into the loin, resulting in a rapid increase in salt content and facilitating the swift diffusion of NaCl within the loin. This is consistent with previous studies. By (Pérez-Santaescolástica et al., 2019). In the later stage of dry curing, the rate of NaCl content increase slowed down because NaCl accumulated on the surface

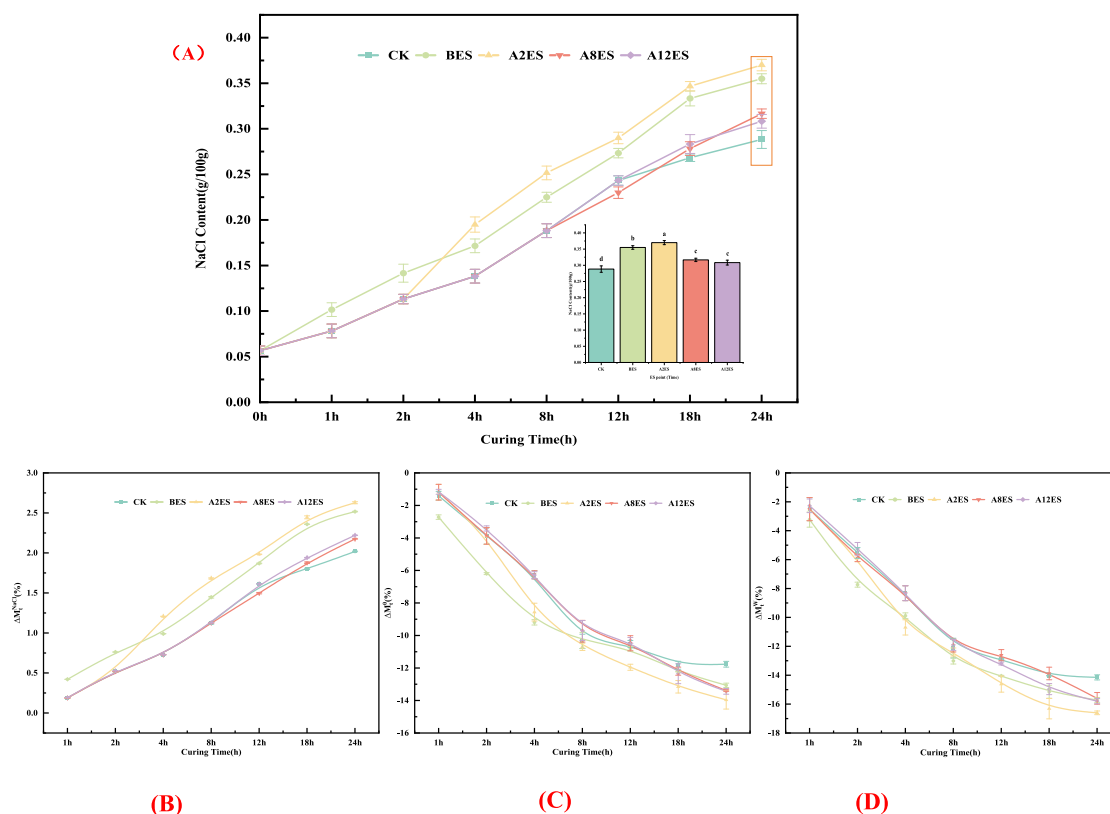


Fig. 2. (A)Electrical stimulation at different time points mediates NaCl content in tenderloin after dry curing. Bars of the insert in (A) with different letters differ significantly ( $p < 0.05$ ). Changes in total weight of pork tenderloin during dry curing: (B) Salt weight change ( $\Delta W_t^{\text{NaCl}}$ ), (C) Total weight change ( $\Delta W_t^0$ ), (D) Water weight change ( $\Delta W_t^w$ ).

of the tenderloin, leading to a gradual decrease in osmotic pressure difference and, consequently, a reduced diffusion rate of NaCl into the meat. Notably, the NaCl content in the BES group was consistently higher than that in the CK group ( $p < 0.05$ ), indicating that ES promoted NaCl diffusion, which is consistent with previous studies (Zhang et al., 2024). After ES was applied at different stages of dry curing, the NaCl content in pork tenderloin was consistently higher than that in the control (CK) and BES groups. This indicates that the combined effects of NaCl curing and ES accelerated the diffusion of NaCl into the meat. The salt content in the A2ES group was the highest, followed by the BES group, while the salt content gradually decreased with the delay in electrical stimulation time ( $p < 0.05$ ). The increase in NaCl content in the electrically stimulated treatment group may be attributed to ES disrupting cell membrane permeability. The excessive current causes cell disruption and widens cellular gaps, allowing external substances to enter the muscle interior. This facilitates salt infiltration and enhances intracellular salt transport (McDonnell et al., 2014; Yue et al., 2024; Zhang et al., 2024). The inset in Fig. 2 (A) shows the NaCl content in the pork loin at the end of the marination process. The NaCl content in pork tenderloin tissue increased by 23.12 % in the BES group, 28.32 % in the A2ES group, 9.82 % in the A8ES group, and 6.94 % in the A12ES group, compared to the CK group. These results indicate that ES-mediated marination enhances the mass transfer process, increases NaCl content in the marinated loin, and improves marination efficiency.

### 3.2. Change in total salt content, total weight, and moisture content

Figs. 2 (B) to (D) illustrate the changes in total salt, total weight, and total moisture content of pork tenderloin during dry curing, reflecting the impact of electrical stimulation on the mass transfer processes within the tenderloin. As illustrated in Fig. 2 (B), the total salt content in the tenderloin blocks increased with marination under all conditions. Notably, the ES treatment significantly accelerated NaCl diffusion, resulting in a markedly higher level ( $p < 0.05$ ) compared to the CK group. This is because, during the early stage of curing, the discrepancy in salt concentration between the surface and the interior of the sample was the most pronounced, creating the largest driving force for diffusion. Consequently, the rate of salt diffusion is faster, leading to a more pronounced change in salt content. Additionally, Crobotova, Tappi, Genovese, Rocculi, Dalla Rosa, and Rustad (2021) found that electric field pre-treatment (0.6 and 0.3 kV/cm) reduced the marinating time of sea bass fillets and increased NaCl uptake (up to 77 %) after electric field treatment, which aligns with the patterns observed in this study.

Fig. 2 (C) illustrates a significant decline in the rate of change in the weight of the tenderloin blocks, attributable to the osmotic dehydration effect and salt-induced protein denaturation. This leads to a rapid loss of water from myofibrillar proteins in the tenderloin and a concurrent reduction in protein solubility, which affects the rate of change in the total weight of the tenderloin blocks (Nguyen et al., 2011). The accelerated deterioration observed in the ES group can be attributed to the combined effects of increased current exposure and NaCl-induced protein degradation. These factors disrupt the protein skeleton, which is essential for maintaining cellular structure. Consequently, changes in the protein microstructure lead to the leakage of cellular contents (Rodrigo et al., 2010).

Fig. 2 (D) illustrates that the rate of change in moisture content decreases with increasing dry curing time. This decline contributes to the observed reduction in the rate of change in total weight. The reduction in moisture content is due to the significant concentration differential between the interior and exterior of the meat, which maintains equilibrium between internal and external ionic concentrations through continuous water loss. Furthermore, the denaturation and salting processes of proteins are intensified, leading to a decreased water-holding capacity within the meat block and significantly accelerating water loss. Concurrently, ES causes the myofibrils to contract, which forces a larger volume of sarcoplasm to remain outside the myofibrils. This

results in reduced space and amount of water available for movement (Hu et al., 2021).

### 3.3. Cell disintegration

The cell disintegration index is calculated by measuring the change in conductivity resulting from the electroporation of the food material after treatment with electric current (Asavasanti et al., 2010). Fig. 3 (A) illustrates the impact of ES on the cell disintegration index (Z). The findings indicate that ES treatment resulted in an increased cell disintegration index. De Vito et al. (2007) investigated that high-intensity electric field treatment can enhance cell disintegration in apple tissue by achieving a high degree of biofilm disintegration through an electroporation mechanism. Furthermore, Zhang et al. (2022) studied the impact of a voltage of 2.0 kV/cm on the disintegration rate and membrane permeability of beef. Their findings suggest that this voltage can reduce the marinating time of beef. The high current leads to the formation of more and larger gaps and pores in the cell membrane, which also enhances mass transfer during the subsequent curing process.

### 3.4. Mass transfer kinetics

The variation of NaCl content in meat blocks after different stages of ES was investigated using a mass transfer kinetic model. Fig. 3(B) presents the fitted curves for the square root variation of NaCl content in samples after different stages of ES as a function of curing time. The results indicate that the rate of change in total NaCl content gradually increased with marination, with this increase varying significantly and remaining higher than that of the control group. The mass change of NaCl in the meat pieces was higher in the A2ES group than in the other groups, which is consistent with the results shown in Fig. 2(A). Table 1 presents the kinetic parameters ( $k_1$  and  $k_2$ ) and correlation coefficients ( $R^2$ ) for NaCl changes in cured pork at different stages of electrical stimulation. Compared to the control group, the  $k_1$  value of the BES group increased, while the  $k_1$  values of the A2ES, A8ES, and A12ES groups decreased significantly. The kinetic parameter  $k_2$  gradually increased, reaching a maximum value of 0.0758 for the ES group after 2 h of curing. Subsequently, this value exhibited a decreasing trend, which may be attributed to the varying degrees of electrical breakdown effects induced by ES during the curing process (Crobotova, Tappi, Genovese, Rocculi, Laghi, et al., 2021). Zhang et al. (2022) investigated the effect of electric field-assisted marination on NaCl in beef. The results of the mass transfer kinetics showed that both the  $k_1$  and  $k_2$  values of NaCl mass change increased after electric field-assisted marination compared to static marination, which aligns with the findings of this study. This enhancement is primarily due to the electric field treatment increasing the permeability of the cell membrane, thereby potentially facilitating intracellular mass transfer of salt. Furthermore, the high  $R^2$  value indicates a strong linear relationship in the equation, suggesting that the mass transfer kinetic model can effectively predict NaCl changes in pork during the curing process.

### 3.5. Diffusion coefficient of NaCl

Table 1 demonstrates the effective diffusion coefficients ( $De$ ) of NaCl in dry-cured loin samples with different curing treatments, the diffusion coefficient is a subjective reflection of solute diffusion, elucidating the intrinsic dynamics of NaCl migration. The  $De$  of the CK group was  $1.32 \times 10^{-5} \text{ m}^2/\text{s}$ , and the  $De$  of the ES group samples ranged from  $1.56 \times 10^{-5} \text{ m}^2/\text{s}$  to  $2.37 \times 10^{-5} \text{ m}^2/\text{s}$ . The ES group was significantly ( $p < 0.05$ ) higher than the CK group, which was consistent with the trend of NaCl content in Fig. 2(A). Among them,  $De$  had the highest ES-mediated diffusion coefficient of  $2.37 \times 10^{-5} \text{ m}^2/\text{s}$  after 2 h of marination, this may be due to the fact that the difference between internal and external salt concentrations is greatest at the beginning of dry curing, with a faster rate of NaCl diffusion, which is accelerated by the ES treatment,

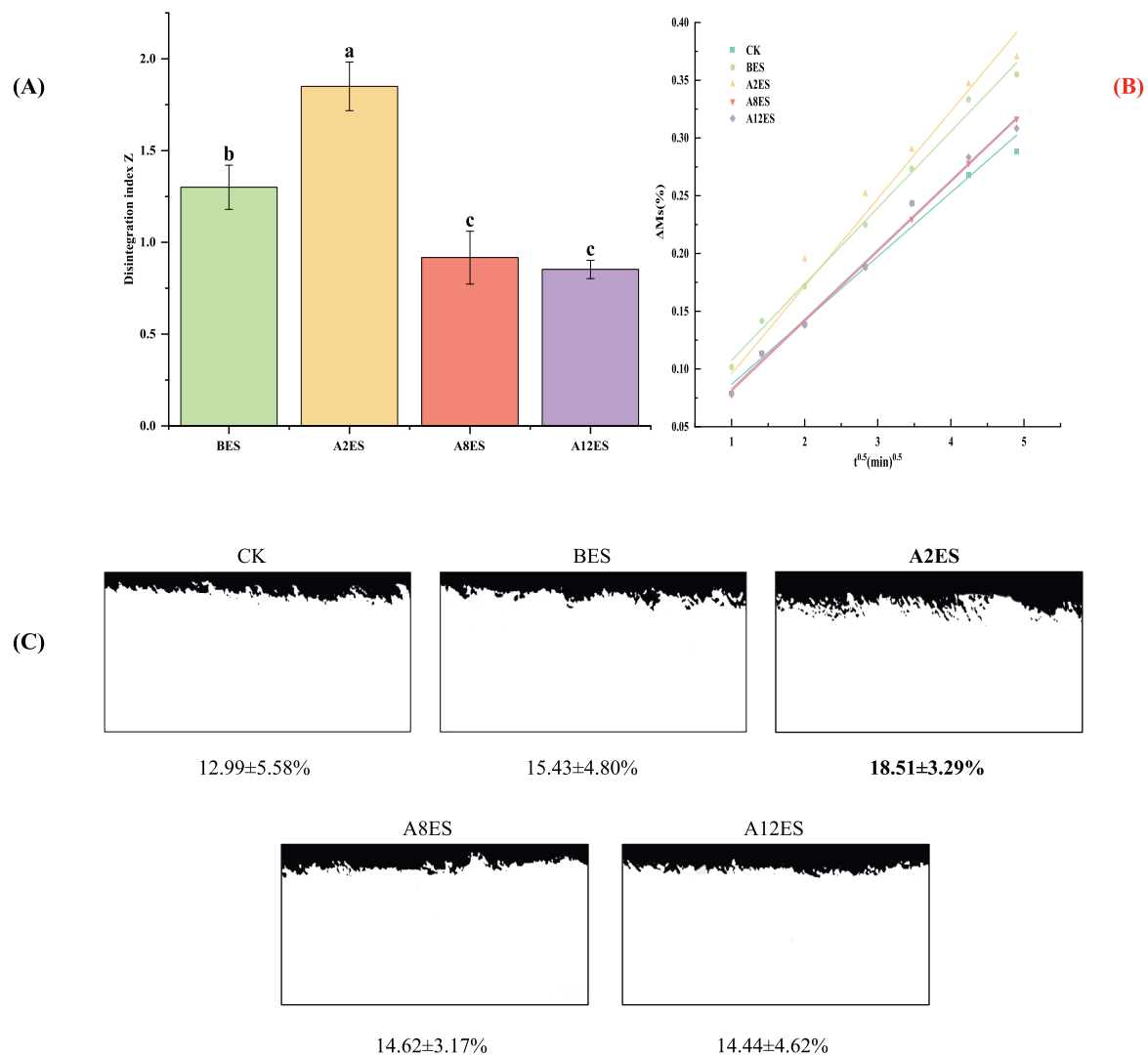


**Fig. 3.** (A) Effect of electrical stimulation on the cell disintegration index Z, with different letters differ significantly ( $p < 0.05$ ). (B) Fitting curve of NaCl content in pork with square root of time after electrical stimulation at different stages of curing. (C) The binarized image of NaCl permeation. Percentage of the black area in the graph indicates the amount of permeable NaCl solution in the pork loin (mean  $\pm$  standard deviation).

**Table 1**

Kinetic parameters and diffusion coefficients of NaCl in tissues of ES cured pork loin.

Curing treatments	$k_1$	$k_2$	$R^2$	Diffusion coefficient ( $10^{-5} \text{ m}^2/\text{s}$ )	K	$R^2$
CK	0.0315	0.0553	0.982	$1.32 \pm 0.11^d$	1.5431	0.9849
BES	0.0415	0.0661	0.9749	$1.81 \pm 0.05^b$	1.4953	0.9928
A2ES	0.0201	0.0758	0.9749	$2.37 \pm 0.16^a$	1.6272	0.9851
A8ES	0.0207	0.0604	0.9982	$1.65 \pm 0.12^c$	1.6119	0.9895
A12ES	0.0226	0.0602	0.9924	$1.56 \pm 0.01^c$	1.6178	0.9879

Note: Different letters in the same column of treatments represent significant differences at  $p < 0.05$ .

which in turn accelerates the diffusion of  $\text{Na}^+$  and  $\text{Cl}^-$  (Jia et al., 2019). The superimposed effect of NaCl and ES led to an increase in  $D_e$ , whereas the NaCl content in the tenderloin gradually approached the curing equilibrium point as the curing time increased and the ES effect diminished, which explains the gradual decrease in  $D_e$  when ES-mediated was applied after 8 h of curing. In addition, it has been shown that electrical treatment can increase the rate of rehydration of

dried cured cod (Genovese et al., 2022) and affect the distribution of NaCl as well as enhance the mass transfer process.

### 3.6. Permeability of NaCl in pork tenderloins

Diffusion coefficients were calculated to characterize the rate of NaCl permeation in pork loin, based on the average NaCl content. However, the extent of NaCl migration through the meat could not be visualized. Therefore, this study employs a visualization method using dye penetration. This method was used to visualize the diffusive migration of NaCl in muscle tissue. ES-mediated dichotomous changes in NaCl permeation in pork loin after marination are shown in Fig. 3 (C). It can be observed that the permeability of NaCl in CK group after curing is 12.99 %, whereas NaCl permeability ranged from 14.44 % to 18.51 % following ES-assisted marination at different stages, with the highest permeability of 18.51 % in the A2ES group. It was observed that NaCl diffusion in the electrically stimulated groups exhibited a needle-like pattern, with the most pronounced effects seen in the A2ES and BES groups. The results indicated that ES enhanced NaCl diffusion. Pork tenderloin, being a complex material with a porous structure, experiences electroporation and fragmentation of the cell membrane when subjected to high electric currents. This process expels air from the pores

of the pork cells. This facilitates the subsequent entry of NaCl molecules into the micropores, thereby accelerating the rate of NaCl diffusion. Wang et al. (2024) investigated how acupuncture electric field preconditioning of pork enlarges the interstitial space within muscle bundles, alters the properties of myogenic fibers, and causes protein molecules to unfold, thereby exposing them to a larger amount of NaCl. This approach also corroborates the results shown in the disintegration index of the cells in Fig. 2 (A).

### 3.7. EDS combined with SEM observation

To visually observe the effect of ES-mediated curing on the fiber tissue structure of pork and the distribution of NaCl within it, energy dispersive X-ray spectroscopy (EDS) combined with scanning electron microscopy (SEM) was employed to obtain microstructural images of the samples. Fig. 4 (A) presents cross-sectional images of fresh pork tissue (FS) alongside CK and ES-treated tenderloin tissue groups. The FS group displays an intact and tightly packed muscle structure, with a few surface cracks caused by freeze-drying. In contrast, the pork tissues in the CK group show slight structural damage following conventional curing. Following electrical stimulation (ES) treatment, the inter-fiber gaps gradually widened. In the BES group, honeycomb-like cracks appeared, with the A2ES group exhibiting extensive honeycomb cracking and further enlargement and fragmentation of the fiber gaps. These microstructural changes in myofibrils confirm that ES accelerates NaCl diffusion by disrupting cell membrane permeability and inducing the enlargement of the myofibrillar gaps. In addition, Faridnia et al. (2014) found that electrical treatment makes the meat structure more porous. The distribution of NaCl content across the cross-sectional area of pork tissue, as obtained by EDS scanning, is shown in Fig. 4 (B), with red dots representing  $\text{Na}^+$  and green dots representing  $\text{Cl}^-$ . After ES treatment, the NaCl content in the loin was most densely distributed and higher than in the CK group, while the FS group exhibited the lowest NaCl content. Table 2 presents the distribution of the total elemental content in the samples' spectral data. The mass percentages of elemental Na and Cl in the FS, CK, BES, and A2ES groups were as follows: Na (wt%): 0.15, 2.31, 3.77, and 4.24; Cl (wt%): 0.16, 3.93, 5.64, and 6.90, respectively.

**Table 2**

Total number of elemental distribution maps spectra.

elemental	line type	wt%	Wt% Sigma	At.%	groups
C	K-line system	55.40	0.34	61.14	FS
N	K-line system	17.13	0.45	16.21	
O	K-line system	27.17	0.22	22.51	
Na	K-line system	0.15	0.02	0.09	
Cl	K-line system	0.16	0.02	0.06	
total amount	K-line system	100.00	/	100.00	
C	K-line system	69.53	0.36	76.34	CK
N	K-line system	7.65	0.44	7.20	
O	K-line system	16.59	0.15	13.67	
Na	K-line system	2.31	0.03	1.32	
Cl	K-line system	3.93	0.04	1.46	
total amount	K-line system	100.00	/	100.00	
C	K-line system	53.04	0.36	61.14	BES
N	K-line system	15.37	0.46	15.19	
O	K-line system	22.18	0.22	19.19	
Na	K-line system	3.77	0.05	2.27	
Cl	K-line system	5.64	0.06	2.20	
total amount	K-line system	100.00	/	100.00	
C	K-line system	51.92	0.41	60.50	A2ES
N	K-line system	15.12	0.53	15.11	
O	K-line system	21.82	0.25	19.09	
Na	K-line system	4.24	0.06	2.58	
Cl	K-line system	6.90	0.08	2.73	
total amount	K-line system	100.00	/	100.00	

The atomic percentages of elemental Na and Cl (At.%) in the FS, CK, BES, and A2ES groups were as follows: Na (At.%) : 0.09, 1.32, 2.27, and 2.58; Cl (At.%) : 0.06, 1.46, 2.20, and 2.73, respectively. The ES treatment group showed significantly higher values than the CK group ( $p < 0.05$ ). In addition, Jia et al. (2019) found that electric fields can migrate  $\text{Cl}^-$  and  $\text{Na}^+$  in meat. The present study further verifies this result by providing specific elemental content data. The results indicate that ES-mediated pickling enhanced the migration and increased the NaCl content in the ridges, which supports the conclusions drawn from the mass transfer model analysis.

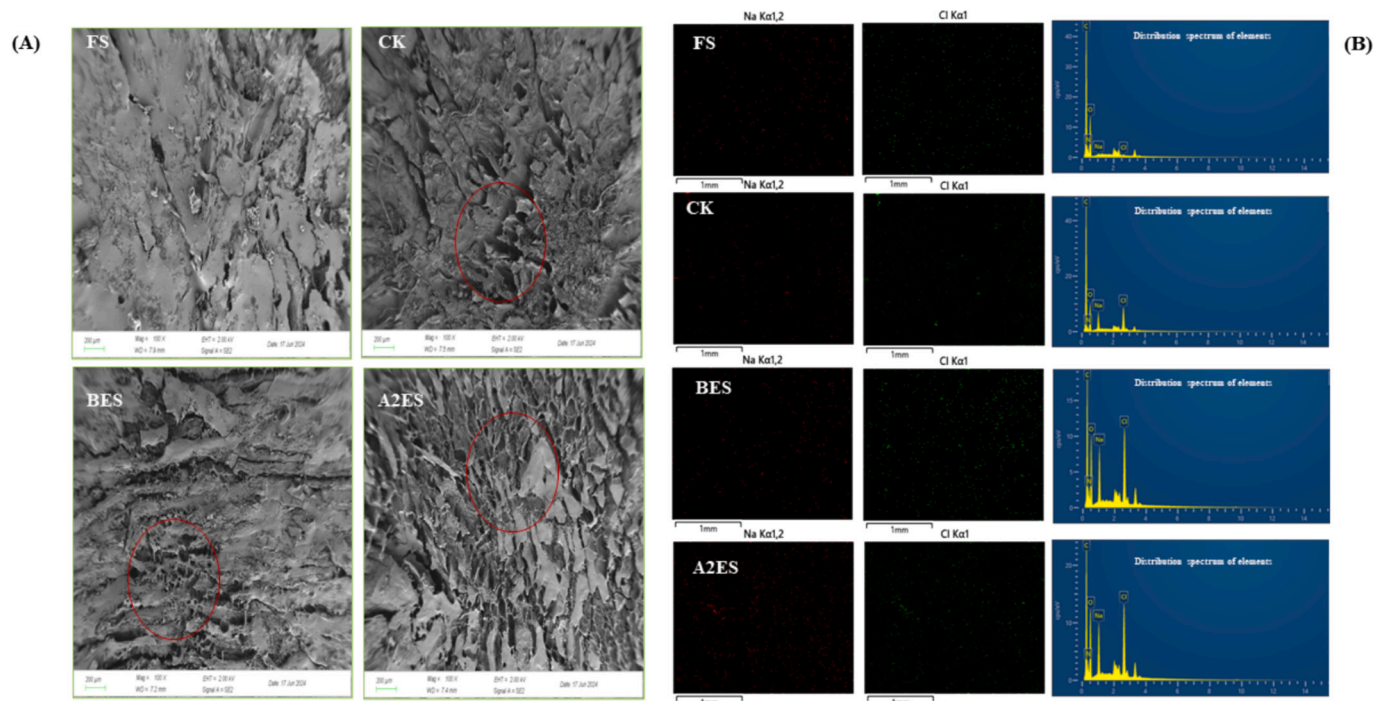


**Fig. 4.** (A) Scanning electron micrographs of cross sections of tenderloin tissues from fresh pork (FS), CK and ES treatment groups, (B) Distribution of NaCl in Pork Tenderloins.

### 3.8. Light microscopic observation

Figs. 5 (A) and 5 (B) illustrate the microstructural changes in both transverse and longitudinal sections of ES-treated pork tenderloin compared to fresh pork tenderloin at different processing times. The results indicated that the myogenic fiber bundles in fresh pork were structurally intact and tightly ordered, with minimal gaps. After ordinary curing, some damage to the tissue structure was observed; NaCl penetrated the muscle, causing partial dissolution of myogenic fibers and expansion of the gaps between adjacent muscle bundles. Following ES treatment, the cross-sectional images of muscle fibers revealed extensive fragmentation and breakage (Ye et al., 2023). The longitudinal sections of the myogenic muscle exhibited increased inter-fiber gaps, with some fiber bundles appearing incomplete. Notably, the A2ES group displayed the most severe muscle tissue damage in cross-section, characterized by twisted lysis of myofibrillar proteins and fragmentation of the myofibrillar structure into varying sizes. This severe damage was primarily attributed to the combined effects of NaCl and ES. After marination, NaCl infiltrates the tenderloin tissue, increasing the ionic strength of the muscle and contributing to the partial proteolysis of certain proteins in the myofibrils. This process, mediated by ES, leads to the physical destruction of the muscle tissue (Hwang et al., 2003).

Additionally, evidence indicates that ES induces the formation of muscle contraction nodes and distortion of muscle fibers, thereby altering the muscle's microstructure (Hughes et al., 2023). This is consistent with the SEM observations.

### 3.9. Analysis of quality characteristics

#### 3.9.1. pH, texture and tenderness

Changes in pH can significantly impact meat quality. As shown in Table 3, ES treatment led to a decrease in pH, but only the last two groups exhibited a significant reduction ( $p < 0.05$ ). This finding is consistent with the study by (Zhang et al., 2019). ES-induced pH decreases have been shown to activate  $\mu$ -calpains, leading to earlier initiation of protein hydrolysis and consequently enhancing muscle tenderness (Hwang & Thompson, 2001).

Regarding texture, the shear force, hardness, and chewiness of the ES-treated dry-cured tenderloin samples were significantly lower than those of the CK group ( $p < 0.05$ ). Regarding elasticity, there was no statistically significant difference except for the A12ES group ( $p > 0.05$ ). These results suggest that post-processing-assisted marination with electrical stimulation has the potential to improve the tenderness and texture of tenderloin.

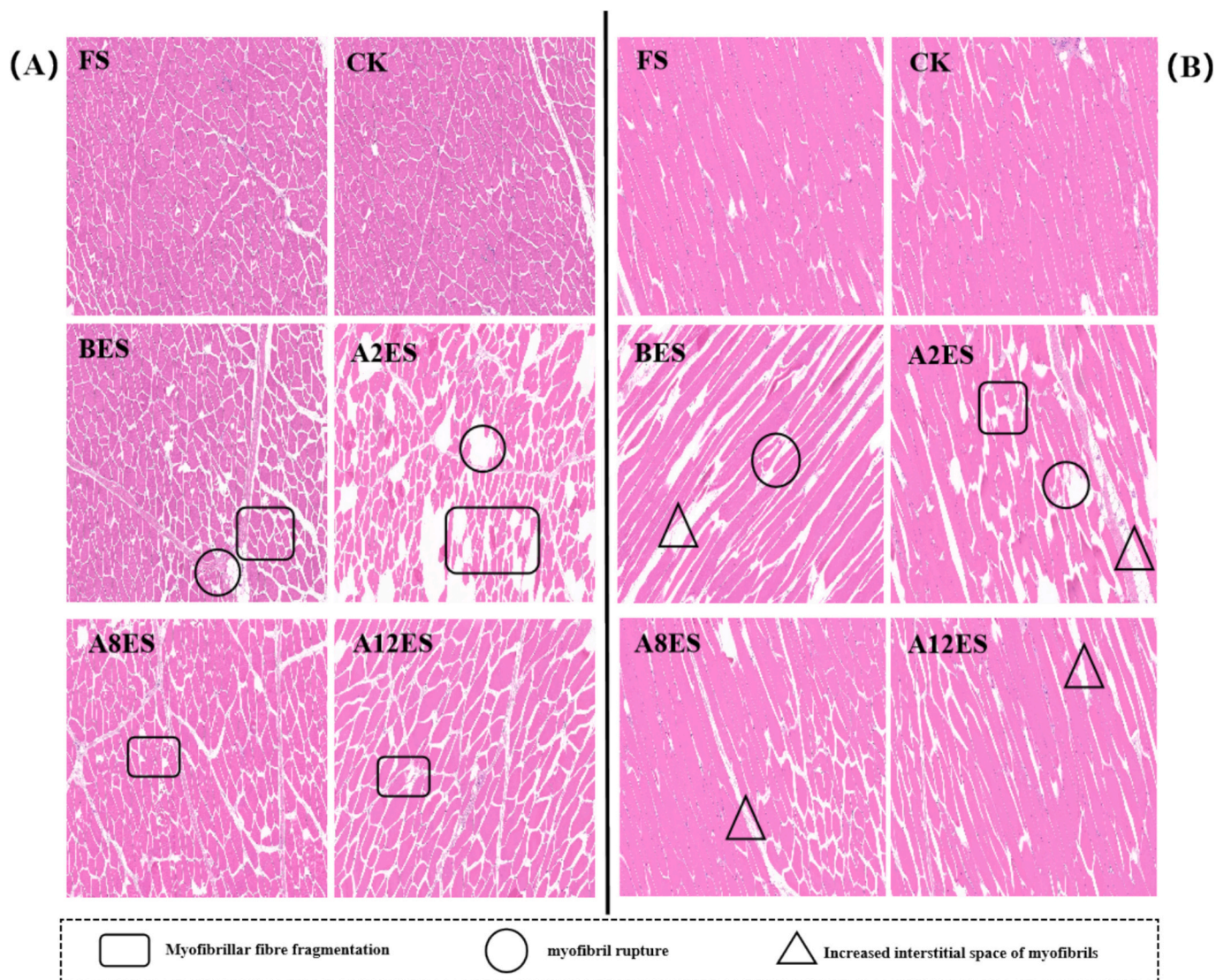


Fig. 5. Microstructural changes in cross-section (A) longitudinal section (B) of ES-treated pork tenderloin compared with fresh pork tenderloin at different processing times. Scale indicates 200  $\mu\text{m}$ .



**Table 3**

Effect of ES-mediated dry curing on pH, shear, textural attributes and color of pork tenderloin after 24 h of curing.

Curing treatments	CK	BES	A2ES	A8ES	A12ES
pH	6.77 ± 0.03 <sup>a</sup>	6.74 ± 0.06 <sup>ab</sup>	6.70 ± 0.06 <sup>abc</sup>	6.67 ± 0.05 <sup>bc</sup>	6.62 ± 0.12 <sup>c</sup>
Shear force (N)	29.20 ± 0.72 <sup>a</sup>	21.98 ± 0.97 <sup>c</sup>	20.06 ± 0.37 <sup>d</sup>	24.61 ± 0.87 <sup>b</sup>	24.05 ± 0.60 <sup>b</sup>
Hardness (gf)	2958.46 ± 14.97 <sup>a</sup>	2319.24 ± 2.06 <sup>c</sup>	1918.55 ± 34.30 <sup>d</sup>	2860.77 ± 24.27 <sup>b</sup>	2359.054 ± 21.98 <sup>c</sup>
Springiness (gf)	0.66 ± 0.02 <sup>ab</sup>	0.69 ± 0.02 <sup>a</sup>	0.69 ± 0.01 <sup>a</sup>	0.67 ± 0.02 <sup>ab</sup>	0.66 ± 0.66 ± <sup>b</sup>
Chewiness (gf)	1236.38 ± 10.33 <sup>a</sup>	969.65 ± 34.23 <sup>d</sup>	863.35 ± 30.52 <sup>c</sup>	1068.67 ± 14.32 <sup>c</sup>	1181.26 ± 14.67 <sup>b</sup>
Lightness (L*)	45.51 ± 0.12 <sup>c</sup>	47.56 ± 0.13 <sup>a</sup>	47.88 ± 0.03 <sup>a</sup>	46.75 ± 0.20 <sup>b</sup>	46.91 ± 0.69 <sup>b</sup>
Redness (a*)	7.22 ± 0.42 <sup>a</sup>	6.42 ± 0.24 <sup>b</sup>	6.16 ± 0.35 <sup>b</sup>	6.09 ± 0.43 <sup>b</sup>	5.96 ± 0.23 <sup>b</sup>
Yellowness (b*)	1.69 ± 0.18 <sup>a</sup>	0.61 ± 0.06 <sup>b</sup>	0.28 ± 0.14 <sup>c</sup>	0.65 ± 0.07 <sup>b</sup>	0.69 ± 0.11 <sup>b</sup>
E*	0.19 ± 0.01 <sup>a</sup>	0.15 ± 0.01 <sup>b</sup>	0.13 ± 0.01 <sup>b</sup>	0.14 ± 0.01 <sup>b</sup>	0.14 ± 0.01 <sup>b</sup>

Note: Different letters in the same column of treatments represent significant differences at  $p < 0.05$ .

Tenderness is a critical factor in determining meat quality; lower shear force values correspond to better tenderness. In the A2ES group, the shear force was reduced by 31.30 % compared to the CK group. ES treatment can enhance tenderness through two mechanisms. First, the electrical current partially disrupts myofibrils and improves NaCl mass transfer and diffusion, causing the myofibrils to relax and swell, thereby increasing tenderness. Second, the current increases cell membrane permeability and damages lysosomes, releasing calcium ions and tissue proteases. The released calcium ions activate calpains, which degrade myofibrils and further improve tenderness (Bhat et al., 2019). The results showed that the use of ES-assisted marination during processing not only did not negatively affect the pH of dry-cured tenderloin, but also showed potential for improving its tenderness and overall quality. Additionally, the enhancement of textural qualities observed in this study may be attributed to the role of ES in promoting mass transfer. This enhanced marination likely induced tenderization by relaxing the muscle structure and causing swelling of myogenic fibers (Bergea et al., 2001).

### 3.9.2. Color changes

Meat color is a crucial indicator for evaluating meat and meat products. As shown in Table 3, the ES treatment significantly ( $p < 0.05$ ) increased the brightness value ( $L^*$ ) while decreasing the redness ( $a^*$ ) and yellowness ( $b^*$ ) values. Although the yellowness value exhibited a trend of initially decreasing and then increasing, this variation was not statistically significant between treatment groups ( $p > 0.05$ ). The increase in the  $L^*$  value is attributed to the electrical breakdown effect induced by ES, which facilitates the diffusion and accumulation of NaCl, thereby enhancing light reflectivity (Bak et al., 2012). The reduction in  $a^*$  is caused by the oxidation of myoglobin to methemoglobin due to high current treatment, which results in a decrease in the redness value (Crobotova, Tappi, Genovese, Rocculi, Laghi, et al., 2021). A decrease in  $E^*$  was observed in the ES treatment, but the difference between treatment groups was not statistically significant ( $P > 0.05$ ). In summary, this suggests that the ES treatment does not produce organoleptic differences in the color of the tenderloin.

### 3.9.3. Electronic tongue analysis

Fig. 6 displays the electronic tongue sensory scores for dry-cured loin treated with ES, as assessed by the taste sensing system. The evaluation included sour, salty, fresh, post-bitter, post-astringent, astringent, and bitter flavors. The most notable difference between the treatment groups

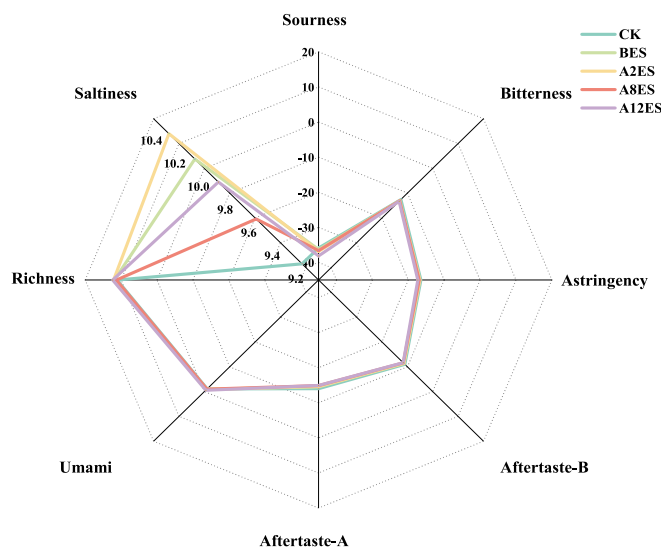


Fig. 6. Dry-cured Pork Tenderloin Electronic Tongue Variations.

was observed in the salty flavor, which aligns with the observed changes in NaCl content. The decrease in acidity correlated with the pH change, though the effect was not significant. Additionally, the ES treatment reduced bitter and astringent flavors, which may be attributed to the reduction of bitter amino acids and the disruption of cellular structure by ES. This disruption accelerates NaCl diffusion, increasing the total NaCl content in the dry-cured loin and inhibiting bitter and astringent flavors (Leighton et al., 2023). Overall, the use of ES at the post-processing stage did not adversely affect the original flavor and even reduced undesirable flavors such as bitterness and astringency.

## 4. Conclusions

The results showed that ES significantly increased the NaCl content in tenderloin at the post-curing processing stage. In particular, the highest NaCl content in the tenderloin was observed under the effect of ES after 2 h of marination, which increased by 28.32 % compared to the CK group. Fick's second law model predicts changes in NaCl content more accurately. The ES treatment significantly increased the diffusion coefficient of NaCl, indicating that the use of ES in the curing process effectively improved the mass transfer during pork curing. The cell disintegration index of ES-treated loin meat was significantly higher than that of the CK group, suggesting that ES altered the permeability of myofibroblast membranes and accelerated the diffusion of NaCl in loin meat tissues, which was confirmed by binarised images. Na + and Cl- elements were most densely distributed in ES-treated pork, suggesting that ES enhanced the migration of NaCl into the pork. In addition, optical microscopy results confirmed that the combined effect of NaCl and ES exacerbated myogenic fiber breakage. Moreover, the ES treatment improves the tenderness and the quality of the tenderloin, and does not have a negative effect. The application of ES technology in the post-processing stage improves the efficiency of meat curing and has a revolutionary application in the food processing field.

## CRedit authorship contribution statement

**Mixin Zhou:** Writing – original draft, Visualization, Validation, Software, Resources, Project administration, Methodology, Investigation, Formal analysis, Data curation. **Yuanyuan Liu:** Writing – review & editing, Data curation. **Chun Ye:** Writing – review & editing, Conceptualization. **Linggao Liu:** Writing – review & editing. **Li Chen:** Formal analysis. **Lisha Lan:** Writing – review & editing. **Shenghui Bi:** Data curation. **Yehua Liu:** Writing – review & editing. **Keshan Wang:**

Writing – review & editing. **Minfei Liu**: Writing – review & editing. **Qiujin Zhu**: Writing – review & editing, Supervision, Project administration, Funding acquisition, Conceptualization.

### Declaration of competing interest

The authors declare that they have no known competing financial interests or personal relationships that could have appeared to influence the work reported in this paper.

### Acknowledgments

This study was funded by the National Natural Science Foundation Project, China (No. 32272359).

### Data availability

Data will be made available on request.

### References

- Asavasanti, S., Ersus, S., Ristenpart, W., Stroeve, P., & Barrett, D. M. (2010). Critical electric field strengths of onion tissues treated by pulsed electric fields. *Journal of Food Science*, 75(7), E433–E443. <https://doi.org/10.1111/j.1750-3841.2010.01768.x>
- Bak, K. H., Lindahl, G., Karlsson, A. H., Lloret, E., Ferrini, G., Arnau, J., & Orlien, V. (2012). High pressure effect on the color of minced cured restructured ham at different levels of drying, pH, and NaCl. *Meat Science*, 90(3), 690–696. <https://doi.org/10.1016/j.meatsci.2011.10.015>
- Bergea, P., Ertbjerg, P., Larsen, L. M., Astruc, T., & Xavier Vignona, A. J. M. (2001). Tenderization of beef by lactic acid injected at different times post mortem. *Meat Science*, 57(4), 347–357. [https://doi.org/10.1016/S0309-1740\(00\)00110-8](https://doi.org/10.1016/S0309-1740(00)00110-8)
- Bhat, Z. F., Morton, J. D., Mason, S. L., & Bekhit, A. E.-D. A. (2019). Pulsed electric field operates enzymatically by causing early activation of calpains in beef during ageing. *Meat Science*, 153, 144–151. <https://doi.org/10.1016/j.meatsci.2019.03.018>
- Biffin, T. E., Smith, M. A., Bush, R. D., Collins, D., & Hopkins, D. L. (2018). The effect of combining tenderstretching and electrical stimulation on alpaca (*Vicugna pacos*) meat tenderness and eating quality. *Meat Science*, 145, 127–136. <https://doi.org/10.1016/j.meatsci.2018.06.002>
- Cropotova, J., Tappi, S., Genovese, J., Rocculi, P., Dalla Rosa, M., & Rustad, T. (2021). The combined effect of pulsed electric field treatment and brine salting on changes in the oxidative stability of lipids and proteins and color characteristics of sea bass (*Dicentrarchus labrax*). *Heliyon*, 7(1), Article e05947. <https://doi.org/10.1016/j.heliyon.2021.e05947>
- Cropotova, J., Tappi, S., Genovese, J., Rocculi, P., Laghi, L., Dalla Rosa, M., & Rustad, T. (2021). Study of the influence of pulsed electric field pre-treatment on quality parameters of sea bass during brine salting. *Innovative Food Science & Emerging Technologies*, 70, Article 102706. <https://doi.org/10.1016/j.ifset.2021.102706>
- De Vito, F., Ferrari, G. I., Lebovka, N. V., Shynkaryk, N., & Vorobiev, E. (2007). Pulse duration and efficiency of soft cellular tissue disintegration by pulsed electric fields. *Food and Bioprocess Technology*, 1(4), 307–313. <https://doi.org/10.1007/s11947-007-0017-y>
- Faridnia, F., Bekhit, A. E. D. A., Niven, B., & Oey, I. (2014). Impact of pulsed electric fields and post-mortem vacuum ageing on beef longissimus thoracis muscles. *International Journal of Food Science & Technology*, 49(11), 2339–2347. <https://doi.org/10.1111/ijfs.12532>
- Genovese, J., Tappi, S., Tylewicz, U., D'Elia, F., De Aguiar Saldanha Pinheiro, A. C., & Rocculi, P. (2022). Dry-salted cod (*Gadus morhua*) rehydration assisted by pulsed electric fields: Modelling of mass transfer kinetics. *Journal of the Science of Food and Agriculture*, 102(11), 4961–4965. <https://doi.org/10.1002/jsfa.11852>
- Graiver, N., Pinotti, A., Califano, A., & Zaritzky, N. (2009). Mathematical modeling of the uptake of curing salts in pork meat. *Journal of Food Engineering*, 95(4), 533–540. <https://doi.org/10.1016/j.jfoodeng.2009.06.027>
- Guo, L., Xu, X., Zhang, X., Chen, Z., He, R., & Ma, H. (2023). Application of simultaneous ultrasonic curing on pork (longissimus dorsi): Mass transport of NaCl, physical characteristics, and microstructure. *Ultrasonics Sonochemistry*, 92, Article 106267. <https://doi.org/10.1016/j.ultrsonch.2022.106267>
- Guo, L., Zhang, X., Guo, Y., Chen, Z., & Ma, H. (2024). Evaluation of ultrasonic-assisted pickling with different frequencies on NaCl transport, impedance properties, and microstructure in pork. *Food Chemistry*, 430, Article 137003. <https://doi.org/10.1016/j.foodchem.2023.137003>
- Hu, F., Qian, S., Huang, F., Han, D., Li, X., & Zhang, C. (2021). Combined impacts of low voltage electrostatic field and high humidity assisted-thawing on quality of pork steaks. *Lwt*, 150, Article 111987. <https://doi.org/10.1016/j.lwt.2021.111987>
- Hughes, J., McPhail, N., Watkins, P., Stark, J., Warner, R. D., & Purchas, R. (2023). Increased light scattering in electrically stimulated beef longissimus muscle fibres contributes to the observed meat colour at grading. *Animal Production Science*, 63(7), 673–680. <https://doi.org/10.1071/an22390>
- Hwang, I. H., Devine, C. E., & Hopkins, D. L. (2003). The biochemical and physical effects of electrical stimulation on beef and sheep meat tenderness. *Meat Science*, 65(2), 677–691. [https://doi.org/10.1016/S0309-1740\(02\)00271-1](https://doi.org/10.1016/S0309-1740(02)00271-1)
- Hwang, I. H., & Thompson, J. M. (2001). The effect of time and type of electrical stimulation on the calpain system and meat tenderness in beef longissimus dorsi muscle. *Meat Science*, 58(2), 135–144. [10.1016/S0309-1740\(00\)00141-8](https://doi.org/10.1016/S0309-1740(00)00141-8)
- Janositz, A., Noack, A. K., & Knorr, D. (2011). Pulsed electric fields and their impact on the diffusion characteristics of potato slices. *LWT - Food Science and Technology*, 44(9), 1939–1945. <https://doi.org/10.1016/j.lwt.2011.04.006>
- Jia, G., Sha, K., Meng, J., & Liu, H. (2019). Effect of high voltage electrostatic field treatment on thawing characteristics and post-thawing quality of lightly salted, frozen pork tenderloin. *Lwt*, 99, 268–275. <https://doi.org/10.1016/j.lwt.2018.09.064>
- Lebovka, N. I., Bazhal, M. I., & Vorobiev, E. (2002). Estimation of characteristic damage time of food materials in pulsed-electric fields. *Journal of Food Engineering*, 54(4), 337–346. [https://doi.org/10.1016/S0260-8774\(01\)00220-5](https://doi.org/10.1016/S0260-8774(01)00220-5)
- Leighton, P. L. A., López-Campos, Ó., Chabot, B., Scott, H. R., Zawadski, S., Barragán-Hernández, W., et al. (2023). Impact of a constant current electrical stimulation (CCES) system and hormonal growth-promoting (HGP) implants on meat quality and palatability of finished steers. *Meat Science*, 205, Article 109297. <https://doi.org/10.1016/j.meatsci.2023.109297>
- Liu, L., Zhou, Y., Wan, J., Zhu, Q., Bi, S., Zhou, Y., et al. (2022). Mechanism of polyhydroxy alcohol-mediated curing on moisture migration of minced pork tenderloin: On the basis of molecular docking. *Food Chemistry: X*, 15, Article 100401. <https://doi.org/10.1016/j.fochx.2022.100401>
- Liu, Z., Xiong, Y. L., & Chen, J. (2010). Protein oxidation enhances hydration but suppresses water-holding capacity in porcine longissimus muscle. *Journal of Agricultural and Food Chemistry*, 58(19), 10697–10704. <https://doi.org/10.1021/jf102043k>
- McDonnell, C. K., Allen, P., Chardonnerau, F. S., Arimi, J. M., & Lyng, J. G. (2014). The use of pulsed electric fields for accelerating the salting of pork. *LWT - Food Science and Technology*, 59(2), 1054–1060. <https://doi.org/10.1016/j.lwt.2014.05.053>
- Nguyen, M. V., Arason, S., Thorarindottir, K. A., Thorkelsson, G., & Gudmundsdóttir, A. (2010). Influence of salt concentration on the salting kinetics of cod loin (*Gadus morhua*) during brine salting. *Journal of Food Engineering*, 100(2), 225–231. <https://doi.org/10.1016/j.jfoodeng.2010.04.003>
- Nguyen, M. V., Thorarindottir, K. A., Gudmundsdottir, A., Thorkelsson, G., & Arason, S. (2011). The effects of salt concentration on conformational changes in cod (*Gadus morhua*) proteins during brine salting. *Food Chemistry*, 125(3), 1013–1019. <https://doi.org/10.1016/j.foodchem.2010.09.109>
- Ozuna, C., Puig, A., García-Pérez, J. V., Mulet, A., & Cárcel, J. A. (2013). Influence of high intensity ultrasound application on mass transport, microstructure and textural properties of pork meat (longissimus dorsi) brined at different NaCl concentrations. *Journal of Food Engineering*, 119(1), 84–93. <https://doi.org/10.1016/j.jfoodeng.2013.05.016>
- Pérez-Santaescolástica, C., Fraeye, I., Barba, F. J., Gómez, B., Tomasevic, I., Romero, A., et al. (2019). Application of non-invasive technologies in dry-cured ham: An overview. *Trends in Food Science & Technology*, 86, 360–374. <https://doi.org/10.1016/j.tifs.2019.02.011>
- Rodrigo, D., Sampedro, F., Silva, A., Palop, A., & Martínez, A. (2010). New food processing technologies as a paradigm of safety and quality. *British Food Journal*, 112(5), 467–475. <https://doi.org/10.1108/00070701011043727>
- Saulis, G. (2010). Electroporation of cell membranes: The fundamental effects of pulsed electric fields in food processing. *Food Engineering Reviews*, 2(2), 52–73. <https://doi.org/10.1007/s12393-010-9023-3>
- Sleper, P. S., Hunt, M. C., Kropf, D. H., Kastner, C. L., & Dikeman, M. E. (2006). Electrical stimulation effects on myoglobin properties of bovine longissimus muscle. *Journal of Food Science*, 48(2), 479–483. <https://doi.org/10.1111/j.1365-2621.1983.tb10771.x>
- Tomac, A., Rodríguez Mallo, S., Perez, S., Garcia Loredo, A. B., & Yeannes, M. I. (2020). Vacuum impregnation in Merluccius hubbsi hake filets brining. Effect on mass transfer kinetics, texture and colour. *Lwt*, 119, Article 108892. <https://doi.org/10.1016/j.lwt.2019.108892>
- Wang, Y., Tao, Y., Chen, Q., Dong, Z., Xiong, Q., & Li, X. (2024). Accelerated pork salting using needle electrode-derived pulsed electric fields. *Food Bioscience*, 59, Article 103994. <https://doi.org/10.1016/j.fbio.2024.103994>
- Wu, B., Qiu, C., Guo, Y., Zhang, C., Guo, X., Bouhile, Y., & Ma, H. (2022). Ultrasonic-assisted flowing water thawing of frozen beef with different frequency modes: Effects on thawing efficiency, quality characteristics and microstructure. *Food Research International*, 157, Article 111484. <https://doi.org/10.1016/j.foodres.2022.111484>
- Ye, X., Ye, C., Zhou, Y., Liu, Y., Wan, J., Liu, L., et al. (2023). Systematic studies on improving structural properties of myofibrillar proteins and pork quality based on electrical stimulation. *International Journal of Food Science & Technology*, 58(5), 2258–2269. <https://doi.org/10.1111/ijfs.16340>
- Yue, X., Bi, S., Li, X., Zhang, X., Lan, L., Chen, L., et al. (2024). Electrical stimulation induces activation of mitochondrial apoptotic pathway and Down-regulates heat shock proteins in pork: An innovative strategy for enhancing the ripening process and quality of dry-cured loin ham. *Foods*, 13(11), Article 1717. <https://doi.org/10.3390/foods13111717>
- Zhang, X., Bi, S., Li, M., Yue, X., Wan, J., Zhou, Y., et al. (2024). Study on activation strategy and effect of protease activity during the post-processing stage of dry-cured meat based on electrical stimulation. *Food Control*, 161, Article 110363. <https://doi.org/10.1016/j.foodcont.2024.110363>
- Zhang, Y., Ji, X., Mao, Y., Luo, X., Zhu, L., & Hopkins, D. L. (2019). Effect of new generation medium voltage electrical stimulation on the meat quality of beef

- slaughtered in a Chinese abattoir. *Meat Science*, 149, 47–54. <https://doi.org/10.1016/j.meatsci.2018.11.011>
- Zhang, Y., Wang, R., Wen, Q.-H., Rahaman, A., & Zeng, X.-A. (2022). Effects of pulsed electric field pretreatment on mass transfer and quality of beef during marination process. *Innovative Food Science & Emerging Technologies*, 80, Article 103061. <https://doi.org/10.1016/j.ifset.2022.103061>
- Zhao, G., Bai, X., Tian, W., Ru, A., Li, J., Wang, H., et al. (2022). The effect of shower time, electrolyte treatment, and electrical stimulation on meat quality of cattle longissimus thoracis muscle in cold weather. *Meat Science*, 184, Article 108664. <https://doi.org/10.1016/j.meatsci.2021.108664>